Nanoscale

RSC Publishing

PAPER

View Article Online
View Journal | View Issue

Cite this: *Nanoscale*, 2013, **5**, 991

The therapeutic effect of PEI-$Mn_{0.5}Zn_{0.5}Fe_2O_4$ nanoparticles/pEgr1-HSV-TK/GCV associated with radiation and magnet-induced heating on hepatoma

Mei Lin,[ab] Junxing Huang,[b] Jia Zhang,[a] Li Wang,[a] Wei Xiao,[b] Hong Yu,[b] Yuntao Li,[a] Hongbo Li,[a] Chenyan Yuan,[a] Xinxin Hou,[a] Hao Zhang[a] and Dongsheng Zhang*[ac]

Comprehensive therapy based on the integration of hyperthermia, radiation, gene therapy and chemotherapy is a promising area of study in cancer treatment. Using PEI-$Mn_{0.5}Zn_{0.5}Fe_2O_4$ nanoparticles (PEI-MZF-NPs) as a gene transfer vector, the authors transfected self-prepared pEgr1-HSV-TK into HepG2 cells and measured the expression of the exogenous gene HSV-TK by RT-PCR. The results showed that HSV-TK was successfully transfected into HepG2 cells and the expression levels of HSV-TK remained stable. Besides, PEI-MZF-NPs were used as magnetic media for thermotherapy to treat hepatoma by magnet-induced heating, combined with radiation-gene therapy. Both *in vitro* and *in vivo* results suggest that this combined treatment with gene, radiation and heating has a better therapeutic effect than any of them alone. The apoptotic rate and necrotic rate of the combined treatment group was 51.84% and 15.45%, respectively. In contrast, it was only 20.55% and 6.80% in the radiation-gene group, 7.49% and 3.62% in the radiation-alone group, 15.23% and 7.90% in the heating-alone group, and only 3.52% and 2.16% in the blank control group. The inhibition rate of cell proliferation (88.5%) of the combined treatment group was significantly higher than that of the radiation-gene group (59.5%), radiation-alone group (37.6%) and heating-alone group (60.6%). The tumor volume and mass inhibition rate of the combined treatment group was 94.45% and 93.38%, respectively, significantly higher than 41.28% and 33.58% of the radiation-alone group, 60.76% and 52.18% of the radiation-gene group, 79.91% and 77.40% of the heating-alone group. It is therefore concluded that this combined application of heating, radiation and gene therapy has a good synergistic and complementary effect and PEI-MZF-NPs can act as a novel non-viral gene vector and magnetic induction medium, which offers a viable approach for the treatment of cancer.

Received 26th September 2012
Accepted 21st November 2012

DOI: 10.1039/c2nr32930a

www.rsc.org/nanoscale

It is well known that radiotherapy, chemotherapy, thermotherapy and biotherapy all play roles in cancer treatment. Each of them has its own merits and demerits. For example, while radiotherapy is an effective cancer treatment, it can inflict significant damage on normal tissue. Further, radiotherapy is mainly effective to G2/M phase cells, with little effect on S or G0 phase cells and hypoxic cells, which will sow seeds for tumor recurrence.[1]

In recent years, many new gene therapies have been explored for treatment of cancer, in which the herpes simplex virus type thymidine kinase/ganciclovir (HSV-TK/GCV) system provides the highest efficacy for targeted gene therapy. In this system, thymidine kinase, a suicide gene expressed by HSV-TK, can change the non-toxic drug precursor GCV into toxic drug, which can kill tumor cells in rapid growth by penetrating into cells to block DNA synthesis. In addition, this system can also produce a killing effect on adjacent untransfected cancer cells *via* the bystander effect. Generally, as long as 10% of the cells are transfected with the expression of the target genes, it will display a great killing effect on the whole tumor tissue by mechanisms related to gap junctions and apoptosis.[2,3] Because these kinds of enzymes do not exist in mammals, the precursor drug exhibits very low toxicity or is non-toxic to mammalian cells. However, two key questions must be answered to accomplish comprehensive gene therapy against cancer for a desired curative effect. One is how to ensure safe gene delivery into cells with high transfection efficacy. The other is how to make gene expression efficient and controllable.

Two of the major gene transfer vectors at present, viral vector systems and non-viral vector systems, both have their own pros

[a]*Medical School of Southeast University, No. 87 Dingjiaqiao Road, Nanjing, 210009, Jiangsu Province, China. E-mail: zdszds1222@163.com; Fax: +86 255 771 2900; Tel: +86 25 8 327 2502*

[b]*Taizhou People's Hospital Affiliated to Nantong University, Taizhou, 225300, Jiangsu Province, China*

[c]*Jiangsu Key Laboratory For Biomaterials and Devices, Nanjing, 210009, Jiangsu Province, China*

and cons. The former, the most efficient so far, is not regularly employed in the clinic due to its small gene capacity, poor target specificity, self-immunogenicity, and the serious biosafety risk it presents in particular. Despite avoiding the major security risks, the latter is greatly inferior to the former in transfection efficiency, and meaningful expression of target gene is hardly available in this system. Currently, lipofection and electroporation are the most widely used methods for non-viral vector transfection with high transfection efficiency. However, liposome is highly cytotoxic and can be quickly cleared by serum *in vivo*, which greatly limits its application. The electroporation method is only suitable for transient and stable expression in cells or tissue *in vitro*, but not for transfection *in vivo*. Moreover, a large number of cells will be killed by the electric shocks involved.[4] Therefore, how to break through the gene transfer bottleneck is still a major challenge in the current gene therapy field.

Recently, radiation-gene therapy was developed through combining the merits of both gene therapy and radiotherapy. More specifically, the genes with antitumor effects can be induced to express by radiation therapy, which results in a dual effect of radiation and target genes for treating cancer. Thus, radiation-gene therapy provides a synergistic antitumor role. The promoter of Egr1, a transcription factor regulating early cell growth, can induce the expression of its downstream genes after ionizing radiation, thereby attaining a spatio-temporal regulation on the target gene expression. Notable achievements in radiation-gene therapy have been obtained by exploiting the radiosensitivity of the Egr1 promoter.[5] However, this method has yet to overcome the common problems in gene therapy, *i.e.* how to ensure a safe gene delivery into cells with high transfection efficacy. Moreover, the anoxic microenvironment in solid tumors is likely to curb the induction activity of the radiation promoter.

Encouragingly, recently developed nanotechnology has offered a new means for solving the problem of the gene transfer vector.[6–10] Research on a gene transfer vector based on nanoparticles has attracted wide attention.[11,12] The therapy genes, such as DNA or RNA, wrapped in the nanoparticles or adsorbed on the surface can be uptaken and released into cells. Compared to traditional carriers, the use of nano-vectors for gene transfer has many advantages, including repeated injections, slow release of the genes to effectively extend response time, maintaining effective concentration of the product, improving transfection efficiency and bioavailability of the product, no immunogenicity, no genetic toxicity, no cytotoxicity, and no cell transformation or death. Such vectors have become a new promising carrier system because they retain the advantages of viral and non-viral vectors and remove their disadvantages.[13–17] Particularly, besides the general properties of nanoparticles, the super-paramagnetic effect of magnetic nanoparticle gene transfer vectors will produce highly efficient transfection and directional movement in an external magnetic field, which in turn helps to carry out targeted gene therapy. Moreover, the magnetic nanoparticles can also be used for heat treatment of cancer because of their induction heating in an external magnetic field.

Thermotherapy represents an alternative treatment for cancer. It can kill cancer cells and improves the sensitivity of chemotherapy and radiotherapy, and it can be applied in combination with radiotherapy, chemotherapy and gene therapy to create a synergistic and complementary effect. However, there is an intractable technical difficulty in heating the tumor tissue evenly at a desired temperature, with no damage to normal tissue during thermal treatment. Jordan, *et al.*, devised a new method of tumor thermotherapy by combining magnetic induction heating with nanotechnology, which was named magnetic fluid hyperthermia. This therapy has a targeted positioning function. In other words, in an external magnetic field only the temperature of the tumor tissue containing magnetic nanoparticles rises, whereas normal tissue without magnetic particles is not subject to thermal damage.[18–20]

In some of our previous studies, $Mn_xZn_{1-x}Fe_2O_4$, thermosensitive Mn/Zn/ferrite magnetic nanoparticles, were chemically prepared and used as the magnetic induction media of thermotherapy and chemotherapy to treat liver cancer and cervical cancer, which yielded good results. Meanwhile, the magnetic materials were tuned to have a specific Curie temperature by adjusting the proportion of Zn and Mn to form $Mn_{0.5}Zn_{0.5}Fe_2O_4$ nanoparticles (MZF-NPs). Properly speaking, MZF-NPs are strong magnetic materials below the Curie temperature, which can absorb electromagnetic waves to warm up in an alternating magnetic field. Upon reaching the Curie temperature, they will change into non-magnetic materials, losing the ability to absorb electromagnetic waves and the temperature starts to decrease. After the temperature falls below the Curie temperature, the materials begin magnetic heating again. So cyclically, the temperature is always changing within the range of the Curie temperature set, such as 42–44 °C, which is an effective treatment temperature for tumors, inflicting no damage to normal tissue. It thus successfully resolves the problem of measurement and controllability of temperature in hyperpyrexia treatment, improving the stability and security of thermotherapy.[21,22]

Based on the above, it is conceivable that we can develop a new therapy for cancer by combining MZF-NPs as magnetic media of thermotherapy and as a gene transfer vector with a radiation promoter to strengthen the induction and regulation of the target gene expression.

Notably, small particles, especially magnetic nanoparticles, easily agglomerate. To ensure the homogeneous dispersion of nanoparticles, surface modification is necessary to help them penetrate into cells to act as a good gene transfer vector. As a common powder surface modification agent, PEI, whose monomer (–CH–CH_2–NH_2–) has a good ability to bind DNA and adhere to cells, has an electrostatic repulsion and steric hindrance effect.[23] MZF-NPs with PEI attached to the surface (PEI-MZF-NPs) exhibited better DNA binding, protection and release abilities, low toxicity and high transfection efficiency as compared to those of liposome and electroporation methods.[24]

In the present study, we constructed a eukaryotic recombinant plasmid-pEgr1-HSV-TK and explored a new multiple therapy of hepatoma by combination of thermal treatment,

radiation treatment and gene treatment, using PEI-MZF-NPs as the gene transfection vector and magnet-induced media simultaneously. We provided evidence that this combined therapy offers a new strategy for the treatment of cancer.

1 Materials and methods

1.1 Main materials

Dimethyl sulfoxide (DMSO) purchased from Sigma; agarose purchased from MRI; DMEM medium and fetal bovine serum from Gibco; Thiazolyl blue (MTT) from AMRESCO; PCDNA3.1 from Biotech Co.Ltd. Changsha Ying Run; Annexin V-FITC and PI kit purchased from Invitrogen Corporation; HepG2 cells were provided by the Institute of Biochemistry and Cell Biology, Shanghai Institute of Biological Sciences, Chinese Academy of Sciences.

1.2 Construction and identification of eukaryotic expression plasmids, pEgr1-HSV-TK

1.2.1 PCR amplification of Egr1 promoter segments. Egr1 promoter was inserted into pIRES vector. In the front of the Egr1 promoter, there was a CMV fragment to enhance the expression efficiency of the promoter. The primer sequences were designed according to CMVE-Egr1p template, and CMVE-Egr1p fragments were amplified by PCR.

Egr1-f: 5′-CCGCTCGAGCGACGCGTGATCTTCAATATTGGCCATTAGC-3′,

---MluI: CGACGCGT; **---**XhoI: CCGCTCGAG

Egr1-r: 5′-CCGCTCGAGCTAGCTAGCCCAAGTTCTGCGCGCTGGGAT-3′

---NheI: CTAGCTAGC; **---**XhoI: CCGCTCGAG

Product length = 1152 bp.

1.2.2 Egr1p was subcloned into pCDNA3.1-EGFP. The above CMVE-Egr1p fragments were collected, amplified and subcloned into pCDNA3.1-EGFP on MluI and NheI sites. After transfection, the plasmids were purified and identified by PCR.

Egr1-f: 5′-CCGCTCGAGCGACGCGTGATCTTCAATATTGGCCATTAGC-3′

Egr1-r: 5′-CCGCTCGAGCTAGCTAGCCCAAGTTCTGCGCGCTGGGAT-3′

Product length = 1152 bp.

According to the PCR electrophoresis results, the correct pCDNA3.1-Egr1-EGFP was selected to sequence.

1.2.3 PCR amplification of HSV-TK segments. HSV106 plasmids were used as templates, and HSV-TK fragments were amplified by PCR.

HSVTK-f: 5′-GGAATTCGCCACCTGGCCTCGTACCCCGGCCAT-3′ (EcoRI)

HSVTK-r: 5′-CCGCTCGAGTCAGTTAGCCTCCCCCATCT-3′ (XhoI)

Product length = 1153 bp

1.2.4 Construction of pcDNA 3.1-Egr1p-HSV-TK. The above HSV-TK fragments were collected, amplified and subcloned into pCDNA3.1-Egr1 on EcoRI and XhoI sites to replace EGFP. After transfection, the plasmids pCDNA3.1-Egr1-HSV-TK were purified and identified by PCR.

HSVTK-f: 5′-GGAATTCGCCACCATGGCCTCGTACCCCGGCCAT-3′

HSVTK-r: 5′-CCGCTCGAGTCAGTTAGCCTCCCCCATCT-3′

Product length = 1153 bp

According to the PCR electrophoresis results, the correct pcDNA3.1-Egr1-HSV-TK was selected to make sure that the sequences were aligned correctly.

1.2.5 pcDNA 3.1-Egr1p-HSV-TK was identified by restriction enzyme digestion. The above pEgr1-HSV-TK constructed was cut by MluI, NheI and EcoRI, XhoI respectively, and the correct insertion was examined by agarose gel electrophoresis. Uncut pEgr1-HSV-TK plasmids served as controls.

1.3 Preparation and characterization of PEI-MZF-NPs

MZF-NPs were prepared by the technique of chemical co-precipitation (for details see ref. 21, 22, 25). Its shape was observed by transmission electron microscopy (TEM) (JEM-200CX, Japan).

1.4 Preparation of PEI-MZF-NPs[24,26]

(1) Some MZF-NPs were dissolved in deionized water to make 4% quality percentage of magnetic fluid. (2) The supernatant was discarded after ultrasonic dispersion and high speed centrifugation. (3) The precipitation was resuspended in PBS buffer. (4) After ultrasonic dispersion, PEI was slowly added to (3) to a 1 : 5 mass ratio of PEI and MZF-NPs, then the suspension was fully mixed and shaken in a table concentrator at a constant temperature. (5) Magnetic nanoparticles were separated from the solution by a magnetic separation method. After repeated washing with distilled water and methanol and vacuum drying, PEI-MZF-NPs were obtained (MZF-NPs coated with PEI).

1.5 Heating test of PEI-MZF-NPs *in vitro*

Various doses of PEI-MZF-NPs were dispersed in 5 ml 0.9% NaCl, to concentrations of 1, 5, 8, 10 and 15 g l^{-1}, respectively. After ultrasonic dispersion, the fluids with different concentrations were placed in corresponding flat-bottomed cuvettes. These in turn were placed in a high frequency electromagnetic field (SP-04C, Shenzhen, China), with a distance of 5 mm from the bottom of the cuvette the center of the hyper-thermia-coil. The output frequency was 230 kHz and the output current was 30 A, the heating time was 1 h and the temperature was measured at 5 min intervals. Heating curves were drawn, using the temperature as the ordinate and time as the abscissa.

1.6 Transfection of pEgr1-HSV-TK into HepG2 cells mediated by PEI-MZF-NPs *in vitro*

(1) We diluted the plasmid DNA and PEI-MZF-NPs separately with serum-free culture medium and then mixed them together (the mass ratio of PEI-MZF-NPs to DNA was 40 : 1) for 30 minutes at room temperature to get the pEgr1-HSV-TK/PEI-MZF-NPs compound. (2) The HepG2 cells were seeded in 6-well plates (5×10^5 cells per well) and incubated in routine conditions. About 18 hours later (80% cells were confluent), the

original culture medium was discarded, and the cells were washed twice with PBS and once with serum-free DMEM. (3) Serum-free DMEM with pEgr1-HSV-TK/PEI-MZF-NPs was added to the wells (every well contained 3 μg DNA), and then the plates were returned to the incubator. 5 hours later, the serum-free medium was replaced with fresh serum DMEM medium, and then incubation of the cells was continued. The transected cells were named HepG2/TK.

1.7 Testing the expression of HSV-TK by RT-PCR

After incubation for 24 h, the HepG2/TK cells were exposed to 4 Gy (6 MeV) of X-ray radiation under a linear accelerator (SIEMENS,PRIMUS.HI), and then continued to be cultured at 37 °C in routine conditions. 72 h later, the total RNA of the HepG2/TK cells was extracted. As a blank control, the total RNA of the HepG2 cells was also extracted. GAPDH cDNA was used as an internal reference gene. All reagents and consumables needed for extracting RNA were RNase-free or were soaked in DEPC water. Primer sequences were synthesized by the Shanghai Ying Jun Company.

TK-f: CCCACGCTACTGCGGGTTTAT (153–174);
TK-r: TGTTGGTGCCGGGCAAGGTC (621–602)
The product length = 469 bp
GAPDH-f: 5′-GCCACATCGCTCAGACAC-3′
GAPDH-r: 5′-CATCACGCCACAGTTTCC-3′
The product length = 614 bp

The system reacted according to a one-step RT-PCR method, and the step was carried out by kit specification. 1% agarose gel electrophoresis was used to identify the results.

1.8 The *in vitro* anti-hepatoma effect of the PEI-MZF-NPs/pEgr1-HSV-TK/GCV magnetic composite nano-system associated with radiation and magnetic induction heating

1.8.1 MTT assay of cell growth and proliferation. After transfection as described above and incubation for 48 h, the HepG2/TK cells and HepG2 cells were digested with 0.25% trypsin and diluted into single cell (4×10^5 cells ml^{-1}) with the fresh complete medium respectively, and then were seeded in five culture bottles (5 ml/bottle), grouped as (1) pEgr1-HSV-TK/PEI-MZF-NPs/GCV combined with radiation bottle, short for radiation-gene therapy group; (2) Egr1-HSV-TK/PEI-MZF-NPs/GCV combined with radiation and heating therapy bottle, short for combined treatment group; (3) the radiotherapy-alone group (without transfection); (4) the thermotherapy-alone group (without transfection); and (5) the untransfected HepG2 cells group, served as a blank control. After incubation for 24 h, GCV with 5 μg ml^{-1} of the ultimate concentration was added to the radiation-gene therapy group and the combined treatment group. PEI-MZF-NPs with 10 g l^{-1} of the ultimate concentration were added to the thermotherapy-alone group and the combined treatment group. The same volume of DMEM culture fluid was added to radiotherapy-alone group and the blank control group. The groups related to radiation were exposed to 4 Gy (6 MeV) of X-ray radiation under a linear accelerator (SIEMENS, PRIMUS.HI, Germany) and the thermal therapy bottles were heated for 1 h on a high frequency heater coil plate (4 kW, 30 A). Then these bottles were continued to be cultured at 37 °C in routine conditions. 48 h later, the cells in each bottle were digested with 0.25% trypsin and diluted into a single cell with all their corresponding original culture medium, and then some of them were subcultured in 96-well plates (200 μl per well) and incubated in air containing 5% CO_2 at 37 °C. 6 wells were repeatedly carried out in every group. 24 h later, 20 μl (5 g l^{-1}) of MTT was added to the cells in each well and continued to be incubated for 4 h. The culture medium was replaced with 150 μl of DMSO and vibrated for 10 min. Then the optical density (OD) values were measured at a wavelength of 493 nm using a microplate reader (Multiskan MK3-353, USA). The cell proliferation inhibition ratio was calculated using the following formula: proliferation inhibition ratio (%) = (1 − OD of the experimental group/OD of the blank control group) × 100%.

1.8.2 Flow cytometry assay. 2×10^6 cells in each group were harvested respectively. After washing with PBS, the supernatant in each group was decanted and the cell pellet was resuspended in 100 μl Annexin-V-Fluos labeling solution which contained 2 μl of Annexin-V-Fluos and 2 μl of Propidium iodide (PI). Cells were incubated for 15 min without light at 25 °C, and then were analyzed on a flow cytometer (FCM, Vantage SE, BD Company, USA) within 1 h.

1.8.3 Cell morphological examination. For electron microscopy, the surplus cells in the above bottles (no less than 5×10^6) of the combined treatment group and the blank control group were collected and centrifuged at 2500 rpm for 10 min, fixed in 4% glutaraldehyde at 4 °C for 72 h and washed with PBS, then fixed in 1% osmium tetroxide, dehydrated step-wise using acetone after PBS washing, embedded in Epon 812 after permeation, and converged for 12 h at 35 °C, for 24 h at 45 °C, and for 24 h at 60 °C in turn. Finally, the cells were prepared into ultrathin sections (60 nm) and were stained with uranyl acetate and lead citrate, then viewed under a TEM (H 600, Japan).

1.9 Animal experiments

Female BALB/c nude mice, aged 6 weeks, each weighing 20–22 grams, purchased from the Lakes Animal Experimental Center of the Institute of Biochemistry and Cell Biology, Shanghai Institute of Biological Sciences, China, were used for the experiments. The experiments were approved by the Animal Care Committee of Jiangsu Province and were performed in accordance with the institutional guidelines. All the mice were maintained in the Sterile Barrier System of Medical School, Southeast University, China. Exponentially growing HepG2 cells (2×10^6 cells) were injected subcutaneously around the right posterior limb rump.

When tumor diameters reached about 1 cm, mice were divided into five groups of six mice each: (1) blank control group, (2) radiation group, (3) radiation-gene group, (4) MZF nanoparticles magnetic induction heating group, heating group for short, and (5) pEgr1-HSV-TK/GCV/MZF nanoparticles associated with magnetic induction heating and radiation group, combined treatment group for short.

Following a multipoint injection strategy, moving clockwise at the 3, 6, 9, and 12 o'clock points, 1 ml sterile normal saline was

injected into the tumors of group (1), and some pEgr1-HSV-TK/MZF/GCV nano-sized compound (MZF: 5 mg/mouse. GCV: 5 mg/mouse. pEgr1-HSV-TK: 10 μg/mouse) was injected into the tumors of group (3) and (5). The tumors of group (2), (3) and (5) were exposed to 8 Gy (6 MeV) of X-ray radiation under a linear accelerator (SIEMENS, PRIMUS.HI, Germany), and the tumors of groups (4) and (5) were heated on a high frequency heater coil plate (4 kW, 230 kHz) for 1 h. The tumor temperature was measured at multipoint using an infrared thermometer (ZyTemp-TN18 model, China). Mice were sacrificed after 6 weeks, and the mass and volume of each tumor were measured. Tumor growth inhibition was evaluated by measuring mass and volume inhibition proportions. Mass inhibition (IM) was calculated as (1 − relative tumor mass) × 100%, where relative tumor mass (RTM) was the mean tumor mass of the experimental group divided by the mean tumor mass of the blank control group. Similarly, volume inhibition (IV) was calculated as (1 − relative tumor volume) × 100%, where relative tumor volume (RTV) was the mean tumor volume of the experimental group divided by the mean tumor volume of the blank control group.

1.10 Statistical analysis

Values were shown as mean ± SD. The data were analyzed with the SPSS 16.0 program. A p value of <0.05 was considered significant.

2 Results and discussion

2.1 Identification of pEgr1-HSV-TK plasmid

Theoretically, digestion of the constructed pEgr1-HSV-TK with EcoRI and XhoI should generate a 1153 bp HSV-TK fragment. Similarly, MluI and NheI digestion will lead to a 1152 bp fragment of Egr1. As shown in Fig. 1, the agarose gel electrophoresis of pEgr1-HSV-TK digested with EcoRI, XhoI and MluI, NheI clearly showed a band about 1152 bp in lane 2 and a band about 1153 bp in lane 3, which confirmed the recombinant plasmid of pEgr1-HSV-TK.

2.2 Characteristics of MZF-NPs

Fig. 2 is an image of MZF-NPs acquired by TEM. It shows that they are nearly spherical, about 15–20 nm in diameter and uniform in size.

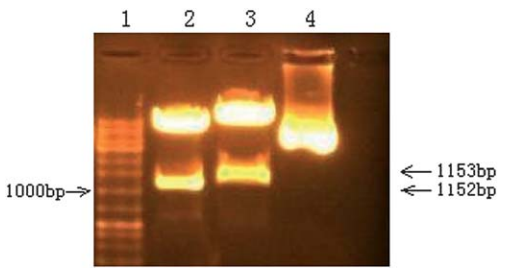

Fig. 1 pEgr1-HSV-TK was identified by restriction enzyme digestion [lane 1: marker (each band in turn from bottom to top is 200, 300, 400, 500, 700, 1000, 2000, 3000, 4000, 5000, 6000 and 10 000 bp); lane 2: pEgr1-HSV-TK was cut by MluI and NheI; lane 3: pEgr1-HSV-TK was cut by EcoRI, XhoI; lane 4: pEgr1-HSV-TK was not cut by any restriction endonucleases].

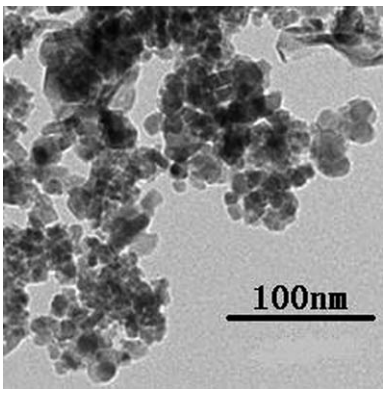

Fig. 2 TEM image of MZF-NPs.

2.3 Heating curve of PEI-MZF-NPs *in vitro*

PEI-MZF-NPs were dispersed in 0.9% NaCl and exposed to a high-frequency alternating electromagnetic field for 60 min. Fig. 3 shows the heating curve of the PEI-MZF-NPs at different concentrations. It was shown that after exposure to the magnetic field, each concentration fluid rapidly warmed, then tended to be stable. As the concentration increased, the maximum temperature rose. Of the tested concentrations, the 10 g l^{-1} solution rapidly warmed within 5 min, then gradually stabilized, and its temperature stabilized at 43 °C or so. This hyperthermia behavior is appropriate for the treatment of tumors because it can stabilize the temperature in the range of tumor therapy while not harming normal tissues. 10 g l^{-1} was thus selected for magnetic induction hyperthermia in the later experiment.

2.4 Gene integration of HSV-TK in HepG2 cells mediated by PEI-MZF-NPs

The mRNA of HSV-TK in HepG2 cells transfected with PEI-MZF-NPs was tested by RT-PCR. The GAPDH gene was used as an internal control so as to rule out any operational error in the PCR process and to determine the quality of TK cDNA amplified. As shown in Fig. 4, two clear genetic fragments with 469 bp and 614 kb, which corresponded to the set length of TK and GAPDH, were obtained in HepG2 cells/TK, whereas there was only one band with 614 kb of GAPDH and no other bands to be

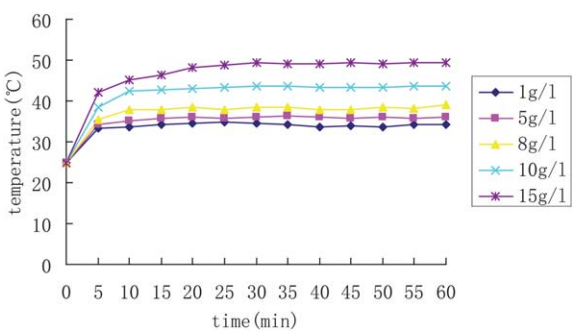

Fig. 3 Heating curve of PEI-MZF-NPs.

seen in the HepG2 cells without transfection. These results suggested that pEgr1-HSV-TK was successfully transfected into HepG2 cells mediated by PEI-MZF-NPs and was able to express stably at the levels of mRNA.

2.5 The therapeutic effect on HepG2 cells treated by a PEI-MZF-NPs/pEgr1-HSV-TK/GCV magnetic composite nano-system combined with radiation and magnetic induction heating *in vitro*

2.5.1 Inhibition of HepG2 cell proliferation tested by MTT. The MTT assay is widely used to examine cell proliferation. The cells of each group with different treatments were incubated over a period of 72 h and the cell viability was determined as described above by MTT. As shown in Table 1, radiation-alone and heating-alone both inhibited HepG2 cell growth, but the combined treatment was markedly superior to any other treatments. The cell proliferation inhibition rate (88.5%) of the combined group with gene, radiation and heating treatment was significantly higher than that of radiation-gene treatment group (59.5%), heating-alone group (60.6%) and radiation-alone group (37.6%).

2.5.2 Flow cytometric analysis of apoptosis and necrosis. The HepG2 cells were stained with Annexin-V-Fluoresce and PI and analyzed by flow cytometry to test whether the growth inhibition in these treatments was caused by apoptosis or necrosis. Generally speaking, in the early stages of apoptosis, changes only occur at the cell surface. One of these plasma membrane alterations is the translocation of phosphatidylserine (PS) from the inner part of the plasma membrane to the outer layer, by which PS becomes exposed at the external surface of the cell, which can be detected by Annexin-V-Fluoresce. Since necrotic cells also expose PS according to the loss of membrane integrity, apoptotic cells have to be differentiated from these necrotic cells. This simultaneous application of a DNA stain which is used for dye exclusion tests allows the discrimination of necrotic cells from the Annexin V positively stained cell cluster. In other words, the single positive of Annexin V stands for apoptosis, and the double positive of Annexin V and PI represents necrosis.

Table 1 Inhibiting effect of different treatments on proliferation of HepG2 cells

Group	Optical density (OD, $\bar{X} \pm s$, $n = 5$)	Proliferation inhibition (%)
Blank control group	1.410 ± 0.052	
Radiation-alone group	$0.881 \pm 0.040^{a,c,e}$	37.6
Radiation-gene group	$0.571 \pm 0.030^{a,b,e}$	59.5
Heat-alone group	$0.556 \pm 0.029^{a,e}$	60.6
Combined treatment group	$0.162 \pm 0.016^{a,b,c,d}$	88.5

[a] $p < 0.001$ *versus* the blank control group. [b] $p < 0.001$ *versus* the radiation-alone group. [c] $p < 0.001$ *versus* the radiation-gene group. [d] $p < 0.001$ *versus* the heat-alone group. [e] $p < 0.001$ *versus* the combined treatment group.

As shown in Table 2 and Fig. 5, apoptosis and necrosis both existed in every treatment group, and the former constituted the major part. Obviously, the combined group with gene, radiation and thermal treatment exhibited better efficacy than any other group. The apoptotic rate and necrotic rate of the combined group was respectively 51.84% and 15.45%. In contrast, it was only 20.55% and 6.80% in the radiation-induced gene group, 7.49% and 3.62% in the radiation-alone group, 15.23% and 7.90% in the heating-alone group, and only 3.52% and 2.16% in the blank control group.

2.5.3 Cell ultrastructural examination. Characterized by active cellular suicide, an apoptotic cell is often associated with such characteristics as chromatin margination, nuclear fragmentation, cytoplasmic blebbing and internucleosomal fragmentation of DNA. The observation of ultrastructural changes demonstrated that PEI-MZF-NPs/pEgr1-HSV-TK/GCV magnetic composite nano-system combined with radiation and magnetic induction heating definitely induced apoptosis of HepG2 cells. Under TEM, we saw many cells in the combined group exhibited morphological features typical of apoptotic cells such as chromatin condensation and chromatin margination or cleavage, and apoptotic body formation. Fig. 6A and B show two TEM pictures of cells treated by radiation, gene and heating together for 48 h. In contrast, most cells in the blank control group were regular in shape with intact nuclei, fine chromatin, and a large, clear nucleolus as shown in Fig. 6C.

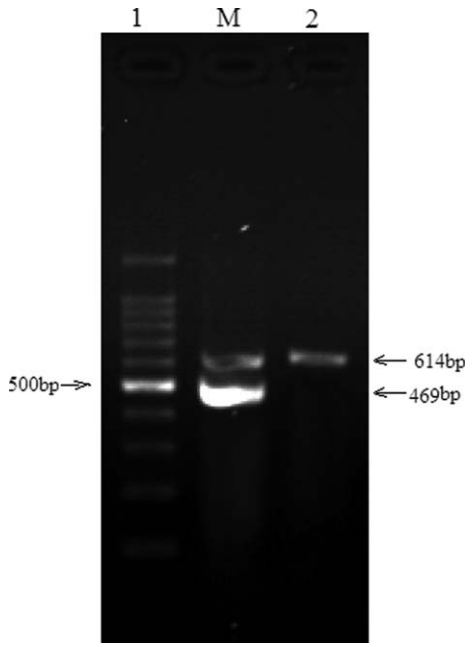

Fig. 4 Gel electrophoresis of HSV-TK amplified by PCR after pEgr1-HSV-TK transfected into HepG2 cells. Lane 1: marker (each band in turn from top to bottom is 7K, 5.5K, 3.5 K, 2 K, 1 K, 600 bp, 500 bp); lane M: HepG2 cells transfected with pEgr1-HSV-TK group with two clear strips, 469 bp of HSV-TK and 614 bp of GAPDH used as reference gene; lane 2: untransfected HepG2 cells group with only one strip, 614 bp of GAPDH.

2.6 *In vivo* anti-hepatoma effect of the PEI-MZF-NPs/pEgr1-HSV-TK/GCV magnetic composite nano-system associated with radiation and magnetic induction heating

To avoid liquid overflow, to ensure fluid dispersion in tumor tissues, and to transfect the whole tumor cells as far as possible,

Table 2 Flow cytometric analysis of apoptosis and necrosis in different therapy groups (%)

Group	Annexin V	Annexin V and PI	Total of apoptosis and necrosis
Blank control group	3.52	2.16	5.68
Radiation-alone group	7.49	3.62	11.11
Radiation-gene group	20.55	6.80	27.35
Heat-alone group	15.23	7.90	23.13
Combined treatment group	51.84	15.45	67.29

we applied a multipoint injection strategy, injecting PEI-MZF-NPs or the PEI-MZF-NPs/pEgr1-HSV-TK/GCV magnetic composite into the 3, 6, 9, and 12 o'clock points of each tumor. After exposure to high frequency AMF (4 kW, 230 kHz) for 30 min, almost the entire tumor was heated by the nanoparticles and the temperature of the tumors rose to 42–45 °C in group (4) and group (5). As shown in Table 3, the therapy of PEI-MZF-NPs/pEgr1-HSV-TK/GCV magnetic composite nano-system associated with radiation and magnetic induction heating greatly inhibited the growth of tumors in nude mice and the effect was much better than that of radiation alone, MZF magnetic induction heating alone or radiation-gene therapy. The tumor volume and mass inhibition rate of group (5) was 94.45% and 93.38%, respectively, significantly higher than the 41.28% and

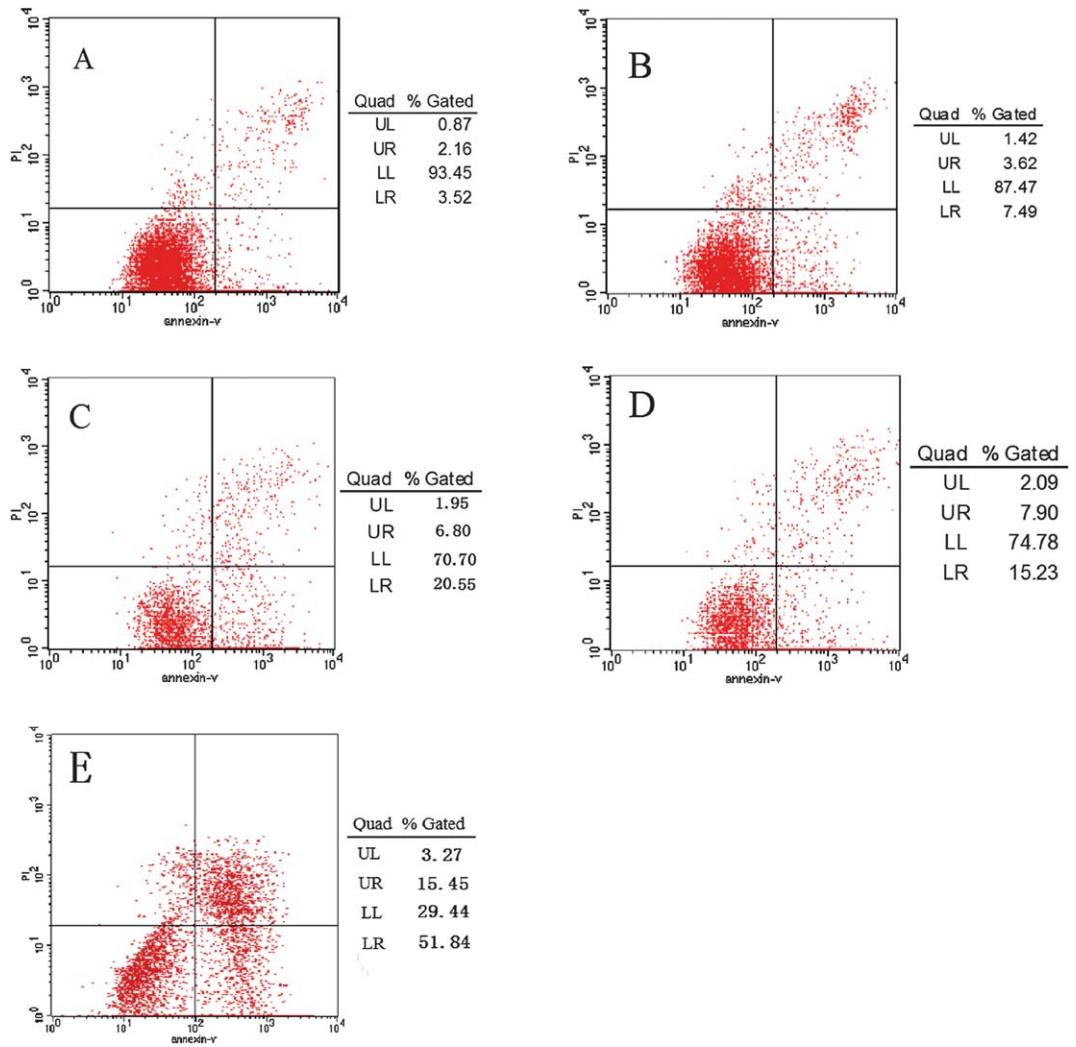

Fig. 5 Apoptosis and necrosis of HepG2 cells analyzed by flow cytometry after different treatments ((A) blank control group. The cell apoptotic rate (AR) and necrotic rate (NR) was respectively 3.52% and 2.16%; (B) radiation-alone group. The AR and NR was respectively 7.49% and 3.62%; (C) radiation-gene group. The AR and NR was respectively 20.55% and 6.80%; (D) heat-alone group. The AR and NR was respectively 15.23% and 7.90%; (E) Combined treatment group. The AR and NR was respectively 51.84% and 15.45%).

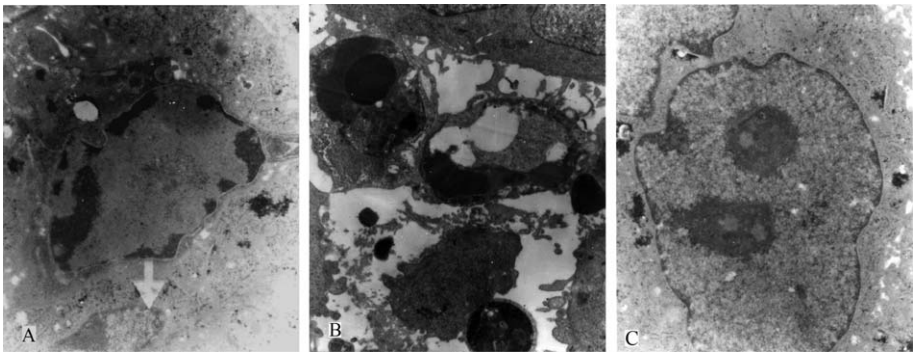

Fig. 6 Ultrastructure of HepG2 cells (observed by TEM). (A and B) Cell treated with radiation, gene and heating therapy together for 48 h. Chromatin condensation, chromatin margination and apoptotic bodies were observed ((A) ×10 000, (B) ×10 000); (C) cell without treatment (×15 000).

33.58% of group (2), the 60.76% and 52.18% of group (3), and the 79.91% and 77.40% of group (4).

The above data indicate that the combined treatment of radiation-gene therapy and magnetic induction heating on cancer, using MZF magnetic nanoparticles as the link, can make a good synergetic effect, reaching 1 + 1 + 1 > 3. It is likely that the mechanisms involve: (1) used as magnetic media of thermotherapy and gene transfer vector, PEI-MZF-NPs perform their own vital functions. (2) High temperature damages the biological integrity of the cell membrane and increases its permeability, which is beneficial to the chemical drug and gene penetration and absorption. (3) Heat restrains repair of DNA fractured by radiotherapy and chemotherapy. (4) While G2 and M phase cells are very sensitive to radiation, S phase cells are very sensitive to heat and temperatures over 42.5 °C can inhibit DNA synthesis and induce lipid peroxidation to wreck cell membrane structure, leading to the tumor cell death. In addition, the therapeutic target of radiotherapy is the DNA of the nucleus, but the thermotherapy target is mainly the cell membrane and cytoskeleton. So the operation of all three combined can overcome their own defects and create a good synergistic and complementary effect. (5) Through improving the cell's metabolism level, heat will help rouse some of the dormant cells in the G0 phase, which are hardly sensitive to both drugs and radiation, into the proliferation stage which then becomes sensitive to radiation and chemotherapy. Additionally, the sensitivity of original proliferative cells is further enhanced. (6) Heating, radiation and genes can take their own cytotoxic effects and kill cancer cells together. (7) Heating can improve expression of the target genes in cancer cells. In addition, cancer tissue is more sensitive to heat than normal tissue, so the former is more likely to die when heated beyond 42.5 °C in the clinic. Low nutrition and low pH provide a conducive environment that increases a cell's sensitivity to heat. Hypoxic cells in solid tumors are often acidic and low-nutrient, so they are more sensitive to thermal damage. Also, heating can improve the tumor's local blood supply and oxygen supply, which helps drugs penetrate into the tumor and increase radiation sensitivity of hypoxic tumor cells.[27] All this serves as a scientific theory and a sound basis upon which further tumor treatment and studies in clinic will be conducted.

3 Conclusions

In this study, we have developed a PEI-MZF-NPs/pEgr1-HSV-TK/GCV composite nano-system. By using PEI-MZF-NPs as gene transfer vectors, we have successfully transfected pEgr1-HSV-TK into HepG2 cells and obtained a sustainable and stable transgenic expression. Moreover, PEI-MZF-NPs have been used as magnetic media for thermotherapy, and an Egr1 promoter has been utilized to strengthen the induction and regulation of HSV-TK gene expression by radiation. Based on the association between radiation and magnetic fluid hyperthermia, gene therapy and nanotechnology are combined organically. Both *in*

Table 3 Volume and mass inhibition of hepatoma in nude mice after different treatments

Group	Tumor volume (mm^3) ($\bar{X} \pm s$, $n = 6$)	Tumor mass (g) ($\bar{X} \pm s$, $n = 6$)	Volume inhibition (%)	Mass inhibition (%)
Blank control group (1)	995.05 ± 132.36	0.801 ± 0.082	0	0
Radiation group (2)	584.28 ± 77.42^{a,c,e}	0.532 ± 0.057^{a,c,e}	41.28	33.58
Radiation-gene group (3)	390.42 ± 39.70^{a,b,e}	0.383 ± 0.034^{a,b,e}	60.76	52.18
Heating group (4)	199.87 ± 34.05^{a,e}	0.181 ± 0.022^{a,e}	79.91	77.40
Combined treatment group (5)	55.25 ± 12.60^{a,b,c,d}	0.053 ± 0.008^{a,b,c,d}	94.45	93.38

^{a} $p < 0.001$ *versus* the blank control group. ^{b} $p < 0.001$ *versus* the radiation group. ^{c} $p < 0.001$ *versus* the radiation-gene group. ^{d} $p < 0.001$ *versus* the heating group. ^{e} $p < 0.001$ *versus* the combined treatment group. These measurements were obtained after treatment for 6 weeks.

vitro and *in vivo* experimental results suggest that this combined treatment provides a far better therapeutic effect than any of the therapies individually. Egr1 can induce the efficient expression of target genes HSV-TK after radiation. It is therefore concluded that PEI-MZF-NPs can be used as a novel non-viral gene vector and magnetic media for thermotherapy which offers a viable approach for treatment of cancer.

4 Disclosure

The authors report no conflicts of interest in this work.

Acknowledgements

The authors extend their sincere thanks to the financial support from National Natural Science Foundation of China (81171452), National Hi-tech Research and Development Program of China (863 project, 2007AA03Z356), Natural Science Foundation of Jiangsu, China (BK2010357), Six Talents Peak Foundation of Jiangsu, China (2011-WS-023), and the key Talent's Foundation in Science and Education, Jiangsu, China (RC2011212), and they would like to express their gratitude to all those who have helped them during the writing of this thesis.

References

1 K. Borgmann, A. Raabe, S. Reuther, S. Szymczak, T. Schlomm, H. Isbarn, M. Gomolka, A. Busjahn, M. Bonin, A. Ziegler and E. Dikomey, The potential role of G2 – but not of G0-radiosensitivity for predisposition of prostate cancer, *Radiother. Oncol.*, 2010, **96**, 19–24.

2 W. F. Anderson, Human gene therapy, *Nature*, 1998, **392**, 25–30.

3 Q. S. Tang, D. S. Zhang, M. L. Wan and L. Jin, Experimental study of the RV-HSV-TK/GCV suicide gene therapy system in gastric cancer, *Cancer Biother. Radiopharm.*, 2007, **22**, 755–761.

4 B. Kealy, A. Liew, J. M. McMahon, T. Ritter, A. O'Doherty, M. Hoare, U. Greiser, E. E. Vaughan, M. Maenz, C. O'Shea, F. Barry and T. O'Brien, Comparison of viral and nonviral vectors for gene transfer to human endothelial progenitor cells, *Tissue Eng., Part C*, 2009, **15**, 223–31.

5 X. J. Xu, L. H. Ding, L. X. Wang, X. Qin, L. Cheng, K. Jiang and Q. N. Ye, Construction of human Egr-1 promoter and its response to ionizing radiation in tumor cells, *Xibao Yu Fenzi Mianyixue Zazhi*, 2009, **25**, 973–975.

6 C. S. Einat, C. Michael, G. Dikla, K. Sivan, K. Nickolay and G. Gershon, Characterization of Monocytes-targeted nanocarriers biodistribution in leukocytes in *ex vivo* and *in vivo* models, *Nano Biomed. Eng.*, 2010, **2**, 91–99.

7 A. Edmund, S. Kambalapally, T. Wilson and R. J. Nicolosi, Dextran-based nanocarriers as efficient media delivery vehicles to cell production bioreactors, *Nano Biomed. Eng.*, 2010, **2**, 126–132.

8 P. Huang, Z. Li, J. Lin, D. Yang, G. Gao, C. Xu, L. Bao, C. Zhang, K. Wang, H. Song, H. Hu and D. X. Cui, Photosensitizer-conjugated magnetic nanoparticles for *in vivo* simultaneous magnetofluorescent imaging and targeting therapy, *Biomaterials*, 2011, **32**, 3447–3458.

9 G. Gao, P. Huang, Y. X. Zhang, K. Wang, W. Qin and D. X. Cui, Gram scale synthesis of superparamagnetic Fe_3O_4 nanoparticles and fluid *via* a facile solvothermal route, *CrystEngComm*, 2011, **13**, 1782–1785.

10 S. Shi, X. C. Zhu, Q. F. Guo, Y. J. Wang, T. Zuo, F. Luo and Z. Y. Qian, Self-assembled triblock copolymer mPEG-PCL-*g*-PEI for co-delivery of drug and DNA: synthesis and characterization *in vitro*, *Int. J. Nanomed.*, 2012, **7**, 1749–1759.

11 Q. F. Guo, T. T. Liu, X. Yan, X. H. Wang, S. Shi, F. Luo and Z. Y. Qian, Synthesis and properties of a novel biodegradable poly (ester amine) copolymer based on poly(L-lactide) and low-molecular-weight polyethyleneimine for gene delivery, *Int. J. Nanomed.*, 2011, **6**, 1641–1649.

12 M. L. Gou, K. Men, J. Zhang, Y. H. Li, J. Song, S. Luo, H. S. Shi, Y. J. Wen, G. Guo, M. J. Huang, X. Zhao, Z. Y. Qian and Y. Q. Wei, Biodegradable heparin conjugated polyethylenimine nano-gel delivering VSVMP gene for C-26 colon carcinoma therapy, *ACS Nano*, 2010, **4**(10), 5573–5584.

13 X. Wang, B. Yu, Y. Wu, R. J. Lee and L. J. Lee, Efficient down-regulation of CDK4 by novel lipid nanoparticle-mediated siRNA delivery, *Anticancer Res.*, 2011, **31**, 1619–26.

14 Y. Liu, T. Wang, F. He, Q. Liu, D. Zhang, S. Xiang, S. Su and J. Zhang, An efficient calcium phosphate nanoparticle-based nonviral vector for gene delivery, *Int. J. Nanomed.*, 2011, **6**, 721–7.

15 M. B. Jesus, C. V. Ferreira, E. Paula, D. Hoekstra and I. S. Zuhorn, Design of solid lipid nanoparticles for gene delivery into prostate cancer, *J. Controlled Release*, 2010, **148**, e89–90.

16 G. Ritu, S. K. Tripathi, S. Tyagi, K. Ravi Ram, K. M. Ansari, P. Kumar, Y. Shukla, D. Kar Chowdhuri and K. C. Gupta, Gellan gum-PEI nanocomposites as efficient gene delivery agents, *J. Biomed. Nanotechnol.*, 2011, **7**, 38–39.

17 H. J. Lee, Y. T. C. Nguyen, M. Muthiah, H. Vu-Quang, R. Namgung, W. J. Kim, M. K. Yu, S. Jon, I. K. Lee, Y. Y. Jeong and I. K. Park, MR traceable delivery of p53 tumor suppressor gene by PEI-functionalized superparamagnetic iron oxide nanoparticles, *J. Biomed. Nanotechnol.*, 2012, **8**, 361–371.

18 A. Jordan, P. Wust, R. Scholz, B. Tesche, H. Fähling, T. Mitrovics, T. Vogl, J. Cervós-Navarro and R. Felix, Cellular uptake of magnetic fluid particles and their effects on human adeno carcinoma cells exposed to AC magnetic fields *in vitro*, *Int. J. Hyperthermia*, 1996, **12**, 705–722.

19 Y. Q. Du, D. S. Zhang, H. Liu and R. S. Lai, Thermochemotherapy effect of nanosized As_2O_3/Fe_3O_4 complex on experimental mouse tumors and its influence on the expression of CD44v6, VEGF-C and MMP-9, BMC Biotechnology, 2009, **9**, 84.

20 S. Y. Yan, D. S. Zhang, N. Gu, J. Zheng, A. W. Ding, Z. Y. Wang, B. L. Xing, M. Ma and Y. Zhang, Therapeutic effect of Fe_2O_3 nanoparticles combined with magnetic fluid hyperthermia on the cultured liver cancer cells and xenograft liver cancers, *J. Nanosci. Nanotechnol.*, 2005, **5**, 1185–1192.

21 J. Zhang and D. S. Zhang, Preparation of a nanosized As_2O_3/$Mn_{0.5}Zn_{0.5}Fe_2O_4$ complex and its anti-tumor effect on hepatocellular carcinoma cells, *Sensors*, 2009, **9**, 7058–7068.

22 L. Wang, J. Zhang, Y. L. An, Z. Y. Wang, J. Liu, Y. T. Li and D. S. Zhang, A study on the thermochemotherapy effect of nanosized As_2O_3/MZF thermosensitive magnetoliposomes on experimental hepatoma *in vitro* and *in vivo*, *Nanotechnology*, 2011, **22**(31), 315102.

23 R. Goyal, R. Bansal, S. Tyagi, Y. Shukla, P. Kumar and K. C. Gupta, 1,4-Butanediol diglycidyl ether (BDE)-crosslinked PEI-*g*-imidazole nanoparticles as nucleic acid-carriers *in vitro* and *in vivo*, *Mol. BioSyst.*, 2011, **7**, 2055–65.

24 M. Lin, D. S. Zhang, J. X. Huang, J. Zhang, L. Wang, T. Guo, L. Xiao, J. Ye and L. X. Zhang, An evaluation on transfection efficiency of pHRE-Egr-1-EGFP in hepatocellular carcinoma cells Bel – 7402 mediated by PEI-MZF-NPs, *J. Nanomater.*, 2011, **2011**, 136052.

25 X. M. Cong, D. S. Zhang and Q. S. Tang, Biocompatibility of $Mn_{0.5}Zn_{0.5}Fe_2O_4$ nanoparticles used in tumor hyperthermia, *J. Southeast Univ., Nat. Sci. Ed.*, 2007, **3**, 23–27.

26 Q. S. Tang, D. S. Zhang and N. Gu, Synthesis and *in vitro* study of PEI-coated MneZn ferrite e a novel gene vector, *J. Funct. Biomater.*, 2007, **38**, 1268e72.

27 L. Zhang, M. Y. Gong, Y. X. Li, L. G. Zhang and X. Y. Wang, Apoptosis of hepatoma cell line HepG2 induced by the combination of radiotherapy and thermotherapy and its relationship with Bcl-2/Bax protein expression, *Chin. Gen. Pract.*, 2011, **14**, 627–630.

